Surface Wetting: From a Phenomenon to an Important Analytical Tool

V. Dutschk

1 Theoretical Concepts of Wetting

Surface wetting as a physical phenomenon has been known for a long time and is the ability of a liquid to keep a contact with a solid surface resulting from intermolecular interactions. The degree of wetting is called *wettability* and is determined by a force balance between adhesive forces, acting between the liquid and solid phases, and cohesive forces, acting in the wetting liquid.

Some 100 years ago, Gibbs [1] elaborated the fundamentals of the thermodynamic theory of capillary; his paper *On the equilibrium of heterogeneous substances* was taken as a basis for all subsequent theoretical and experimental wetting work. Since then, diligent work has been done to describe the wetting behaviour of heterogeneous systems, thereby to determine the surface energies of liquid and solid bodies, and in this manner to predict the adhesion behaviour. Over a period of years, heaps of literature have been accumulated on these problems, proposing various measurement techniques and different evaluation possibilities, including criticism of one or other computational algorithm or fundamental idea.

Following is a brief discussion of the fundamental results.

1.1 Surface Tension and Surface Energy

It is common knowledge that inside a liquid a molecule undergoes a different equilibrium position than at the liquid surface, due to its neighbours, and that work has to be done to direct this molecule toward the surface. As this takes

V. Dutschk (✉)
Engineering of Fibrous Smart Materials (EFSM), Faculty for Engineering Technology (CTW), University of Twente, P.O. Box 217, 7500 AE, Enschede, The Netherlands
e-mail: v.dutschk@utwente.nl

R.G. Rubio et al. (eds.), *Without Bounds: A Scientific Canvas of Nonlinearity and Complex Dynamics*, Understanding Complex Systems,
DOI 10.1007/978-3-642-34070-3_23,

place, the surface will increase by this molecule which now has a potential energy elevated by the amount of this work. The corresponding increase in energy, being related to the unit of area, is referred to as *specific surface energy*. The force needed to do this work and related to the unit of length is referred to as *surface tension*. Most textbooks assume the surface tension to be identical to the specific surface energy. Strictly speaking, these terms are not identical. While the term *surface tension* (a unit of measurement: force per length, the force being determined by specifying amount and direction) originates from classical mechanics, the term *surface energy* (a unit of measurement: energy per area, the energy being fully considered by specifying a number) results from the energy approach. The thermodynamic definition of the surface tension γ expresses it in terms of the change in free energy (F) as the interfacial area (A) of two coexisting phases is changed at constant volume (V)

$$\gamma = \left(\frac{\partial F}{\partial A}\right)_{T,V}. \tag{1}$$

In the theory of capillarity, the surface tension is associated with the tension of two-dimensional membrane located at the boundary between two phases. In the absence of a field, the tensor of excess surface stresses (which is used to introduce the surface tension) is two-dimensional for plane surfaces. However, for a spherical surface, the transverse surface tension appears, i.e. the normal component of the tensor of excess surface stresses, which can be nullified by a simple selection of the position of the dividing surface as a tension surface [2]. In the presence of external field, even such simple as gravitational, the transverse surface tension can hardly be eliminated by some conditional procedures. As a result of the permanent presence of three-dimensional aspect, the theory of interfacial phenomena begins to lose its inherent simplicity and attractiveness.

Liquids with high surface tension, usually reflecting strong intra-molecular bonds, or liquids on low-energy solid surfaces, usually form nearly spherical droplets, whereas liquids with low surface tension, or liquids on high-energy surfaces, usually spread over the surfaces. This phenomenon is a result of minimization of interfacial energy. Thus, if a surface has a high free energy, most liquids will spread on the surface since this will usually lower the free energy. Wetting phenomena have been widely studied both theoretically and experimentally in connection with the physics of surfaces and interfaces.

1.2 Young Equation

Whether a liquid will wet a solid depends on the surface tension of the solid γ_{SG}, that of the liquid γ_{LG}, strictly speaking *interfacial tension* since wetting describes a displacement of a solid–gas (air) interface with a solid–liquid interface, and the interfacial solid–liquid tension γ_{SL}. These quantities are connected with the

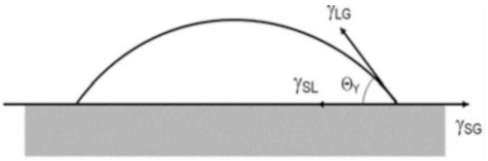

Fig. 1 Liquid drop on a solid surface: Θ_Y is the Young contact angle; γ_{LG} is the interfacial tension liquid–gas; γ_{SG} and γ_{SL} are interfacial tensions solid–gas and solid–liquid, respectively: ideal wetting situation

contact angle Θ_Y by the Young [3] equation where the contact angle stands for the equilibrium angle with the lowest energy state (Fig. 1)

$$\gamma_{SG} = \gamma_{SL} + \gamma_{LG} \cdot \cos \Theta_Y. \tag{2}$$

Since the quantities γ_{SG} and γ_{SL} are generally inaccessible to experiments, as opposed to γ_{LG}, the Young equation is often used for solving the inverse problem, i.e. to determine the difference ($\gamma_{SG} - \gamma_{SL}$, which is referred to as *wetting tension* or *adhesive tension*, by means of the experimental values θ and γ_{LG}. This is the free energy gained when a unit of the solid surface is wetted without changing the size of the liquid surface. The wettability directly depends on the interfacial tension γ_{SL}: the stronger the interfacial interactions, the lower the interfacial tension; the lower the interfacial tension, the better wetting.

1.3 Adsorbed Water Film

Contact angle estimation by means of the Young equation (2) is additionally complicated by the fact that the solid surface is able to adsorb water vapour from the air. The values of γ_{SG} depend on the thickness of the adsorbed water film. Adsorbed layers can change the interfacial behaviour by influencing adhesion due to the adsorption of electrolyte ions. Since water is also a weak electrolyte solution, which often forms a film on "dry" surfaces as an adsorbed layer under normal conditions, research into the relations between surface potentials or surface charges of solids acquires a particular meaning in the presence of an adsorbed water film. Studies in this direction was particularly initiated by Jacobasch [4]. Frumkin, Derjaguin and Churaev [5–8] wetting theory based on the surface forces seems to be best suited in this respect.

Relations between charged surfaces and molecular interaction forces are discussed in the context of this theory. Varying the balance of surface forces, it is possible to control the wetting behaviour. In 1938, Frumkin introduced the term *film tension* γ_f, which is equivalent to the term *solid surface tension* γ_{SG} and depends on the film thickness h [7] as shown in Fig. 2

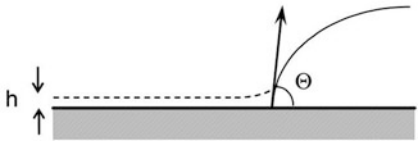

Fig. 2 Schematic representation of a solid surface with a thin wetting film

$$\gamma_f = \gamma_{SG}(h). \tag{3}$$

With a very large h (several hundred nanometers) is valid

$$\gamma_{SG} = \gamma_{SL} + \gamma_{LG}.$$

Assuming that the free energy determination of liquid films is based on a very thick liquid film, with

$$\gamma_f = \gamma_{SL} + \gamma_{LG},$$

rather than on the "dry" solid surface, Frumkin analysed the dependence $\gamma_f = \gamma_f(h)$. From this, the possibility of metastable states of liquid films was obtained with an incomplete wetting situation

$$\gamma_f < (\gamma_{SL} + \gamma_{LG}),$$

and the condition of a complete wetting was defined as

$$\gamma_f \geq (\gamma_{SL} + \gamma_{LG}).$$

At this point, the possible existence of γ_f values was postulated, which exceed the value $(\gamma_{LG} + \gamma_{SL})$ must be emphasised, while the Young equation lacks such a possibility.

1.4 Work of Adhesion

The work of adhesion between liquids and solids is described by the Dupré–Young equation

$$W_A = \gamma_{LG}(1 + \cos\theta). \tag{4}$$

The surface energy of solids can be, at least tentatively, determined by measuring the contact angle.

A different possibility to determine work of adhesion is to represent surface energy as a sum of two components: dispersion component γ_i^d (effect of London dispersion forces) and polar component γ_i^p (due to forces of a different kind). No less than two test liquids (a polar and a non-polar one) have to be used. This method

is based on Fowkes approach [9] which was later converted by Owens and Wendt [10] to the following form

$$\gamma_{12} = \gamma_1 + \gamma_2 - 2\sqrt{\gamma_1^d \cdot \gamma_2^d} - 2\sqrt{\gamma_1^p \cdot \gamma_2^p}.$$

For work of adhesion, hence, follows

$$W_A = 2\sqrt{\gamma_1^d \cdot \gamma_2^d} + 2\sqrt{\gamma_1^p \cdot \gamma_2^p}.$$

The surface tension of solids can be calculated by means of Young equation (2). However, the interfacial tension, γ_{SL} (or γ_{12}), as a result of the interactions between liquid and solid, cannot be determined directly in a wetting experiment. There are approaches which try to bypass the problem.

1.5 Critical Surface Tension

Since the state of surfaces is capable of influencing their wettability Zisman [10] introduced *critical surface tension* γ_c. Zisman examined the linear relation

$$\cos\theta = a - b \cdot \gamma_{LG},$$

with various test liquids. Then, γ_c results by linear extrapolation

$$\gamma_c = \lim_{\theta \to 0} \gamma_{LG}.$$

Measurements with non-polar liquids allow determination of the dispersion component γ_i^d and those with polar liquids determination of the polar one γ_i^p.

Based on the critical surface tension concept, Neumann [11] suggested to estimate surface free energies of solid substrates γ_{SG} from experimentally determined advancing contact angles of a known liquid (e.g. water) using the equation of state for solid–liquid interfacial tension developed in the frames of semi-empirical theory

$$\cos\theta = -1 + 2\sqrt{\gamma_{SG}/\gamma_{LG}} \cdot e^{-0.0001247(\gamma_{LG}-\gamma_{SG})^2}.$$

1.6 Fowkes and Good Theories

Fowkes proposed the possibility of splitting the surface energy into four terms γ_i^d and γ_i^p already mentioned in Sect. 1.4 as well as additional terms γ_i^i and γ_i^H (for

London, Debye, Keesom and hydrogen bond interactions[1]). For determination of the dispersion adhesion energy component, the Fowkes idea leads to the Good–Girifalco approach [12][2]

$$W_A^d = 2\sqrt{\gamma_1^d \cdot \gamma_2^d}. \tag{5}$$

For wetting non-polar liquids such as alkanes on rather non-polar polymers, surface energy is determined only by van der Waals forces: $\gamma_{non-polar} = \gamma^d$.

Fowkes also pointed out that "polar" forces (orientation and induction forces) hardly contribute to work of adhesion if contact formation happens between a polar liquid (i.e. water) and a non-polar liquid or solid surface. To determine the surface energy of polymers one then needs two liquids with the highest possible surface energy and the lowest possible tendency to formation of acid–base bonds, e.g. diiodomethane ($\gamma = \gamma^d = 50.8\,\mathrm{mJ/m^2}$) and 1-bromonaphthalene ($\gamma = \gamma^d = 44.4\,\mathrm{mJ/m^2}$). According to Fowkes, the contribution of Keesom and Debye forces to work of adhesion can be neglected, permitting the whole work of adhesion to be presented as a sum of two components: W_A^d and W_A^{ab}, where W_A^d is the work done by *non-specific* van der Waals forces (mainly by dispersion forces) and W_A^{ab} the work done by *specific* interactions (so-called acid–base interactions).

Contrary to the work done by *non-local* dispersion forces, the component W_A^{ab} of the work of adhesion is due to the formation of *local* donor–acceptor bonds at the interface. Because of its local nature, such an interaction can occur only with a direct contact of both bodies. Furthermore, the adhesion of rather non-polar polymers, such as polyolefin polymers or fluoroplastics, is only caused by the action of the van der Waals forces, whereas the contribution of the acid–base interactions to the total value of the work of adhesion of polar polymers can reach 70–80% [13].

The formation of an electric double layer in the contact area of two solid surfaces due to the formation of donor–acceptor bonds between them is the subject of Derjaguin's semi-empirical electric theory of adhesion [14, 15]. According to it, an exchange of electrons takes place at the contact site, which is due to different electronic structural levels of the contacting material.

Functional groups, such as hydroxyl group OH, carboxyl group COOH, phenyl ring, nitrile group CN, and amino group NH_2, act at the polymer surface as carriers of their adhesion activity much as they determine the mechanical properties of the polymer inside the latter.[3] The relation between the presence of the functional groups and the adhesiveness of some polymer materials is certainly no accident. Based on investigations of the semiconductor-polymer system, Jacobasch and Freitag [16] made up the following succession of donor–acceptor properties of the functional groups contained in polymers:

---

[1] Subsequently, Fowkes used the index "ab" (for *acid–base*) instead of "H". Hydrogen bonding is a special case of acid–base bonding.

[2] This one resulting from calculations according to Lifschitz theory.

[3] E.g. the presence of COOH, OH, or NH_2 groups which interact with polar groups of adjacent chains is responsible for a higher mechanical strength of the polymer.

$$–CN >= CO > –COOR > –C_6H_5 > –OR > –OH > NH_2,$$

where by the donor–acceptor properties change from left (donor) to right (acceptor).

Moreover, the same authors concluded that, in vacuum, the electrostatic component is predominant for the adhesion of polymers. The question was raised by Jacobasch [17] as to the validity of this deduction for actual interacting systems, i.e. for the contact formation in humid atmosphere (whereby conduction of the charge carriers is possible) and it still remains open. Generally speaking, functional groups in polymers may be made up in series according to their donor properties. Each previous member of the series functions as an electron pair donor with regard to the following member, which then acts as an electron pair acceptor.

Combining polymers, which are to interact with one another adhesively according to the acid–base principle, with consideration of the fact that the possibility of a non-symmetric electron density distribution in the contact area grows as the functional groups move away from one another in a series, makes it possible to derive the following empirical rule: to attain a good adhesion, thus great bond strengths, polymers must be purposefully combined with one another in such a way that their functional groups in a donor–acceptor series are as far as possible apart.

In view Fowkes's ideas, Berg called Fowkes a "pioneer" and the latter was highly esteemed for the development of his theory as well as its applications with practical problems of wetting and adhesion [18]. Fowkes' notion of necessary consideration of specific acid–base interactions was improved by Good [19, 20], who assumed that γ^{ab}, again, can be divided into two components by analogy with K_A and K_B constants according to Gutmann [21]: γ^+ (*acidic surface parameter* or Lewis acidic component) and γ^- (*basic surface parameter* or Lewis basic component).

(i) If both components γ^+ and γ^- of a substance can be neglected this substance is referred to as *non-polar* or *inert* (e.g. diiodomethane).
(ii) If either of both components is dominant this substance is defined as *monopolar* or *mono-functional* (e.g. ether).
(iii) If neither of both components can be neglected this substance is referred to as *bipolar* or *bifunctional* (e.g. water).

Table 1 shows that a considerable differences exist between the theoretical and experimental value for surface energy of water and glycerine.

For surface energy of water being a polar liquid, the following results [18] $\gamma^p + \gamma^i = 1.4\,\text{mJ/m}^2$ and $\gamma^d = 21.1\,\text{mJ/m}^2$. The surface energy of water determined experimentally amounts to approximately $73\,\text{mJ/m}^2$. Hence, it follows that the contribution of the specific acid–base interaction to the total surface energy of water comes to $\gamma^{ab} = 73 - (21.1 + 1.4) = 50.5\,\text{mJ/m}^2$. With water both components γ^+ and γ^- are uniform in size [18] $\gamma^+ = \gamma^- = 25.25\,\text{mJ/m}^2$.

Surface energy of chloroform, $CHCl_3$, and that of non-polar tetrachloromethane, CCl_4, are approximately equal ($\gamma = 29\,\text{mJ/m}^2$), work of adhesion with regard to water is, however, different W_A ($CHCl_3/H_2O$) $= 68.3\,\text{mJ/m}^2$ and W_A (CCl_4/H_2O) $= 54.7\,\text{mJ/m}^2$. The difference of $13.7\,\text{mJ/m}^2$ resulting from the formation of hydrogen

Table 1 Hamaker[a] constants and surface energies of some materials, calculated and determined experimentally [22]

Substance	Hamaker constant, $\times 10^{-20}$J	Surface energy γ, mJ/m^2	
		Theoretical	Experimental
Polystyrene (PS)	6.6	32.1	33.0
Polytetrafluoroethylene (PTFE)	3.8	18.5	18.3
Water	3.7	18.0	73.0
Glycerine	6.7	33.0	63.0

[a]The Hamaker constant is a interacting system specific parameter representing Van der Waals interaction between bodies

Table 2 Comparison between the surface energies of PS according to data found in the literature

Surface energy, mJ/m^2	Determination method						
	1	2	3	4	5	6	7
γ^d	42.0			44.0	26.5	26.5	
γ^p					8.1	8.3	
γ^{ab}	1.1						
γ	43.1	42.6	32.8		32.6	34.8	34.9
Reference	[23]	[24]	[25]	[25]	[17]	[17]	[26]

γ^d being the dispersion component, γ^p polar and γ^{ab} acid–base component of the surface energy; γ is the entire surface energy; measurement technique or theoretical approach, respectively: (1) Sessile drop method (geometric mean); (2) Owens–Wendt (harmonic mean); (3) according to Zisman; (4) according to Fowkes; (5) Owens–Wendt (geometric mean); (6) estimated from T_g value; (7) estimated through measuring surface forces between two polystyrene surfaces

bonds between chloroform and water—Cl_3C-H...OH_2—can be interpreted according to these ideas [19].

Surface energy of polystyrene, which is mono-polar, may be presented according to this approach as follows [18] $\gamma^d = 42\,\text{mJ/m}^2$; $\gamma^+ = 0$; $\gamma^- = 1.1\,\text{mJ/m}^2$.

Bibliographical values for the surface energy of polystyrene are summarized in Table 2.

Furthermore, significant non-dispersion contributions to the surface energy were found for polymethylmethacrylate (PMMA), polyvinylchloride (PVC), polyvinylchloride (PET), polyamide (PA 6) and none for polytetrafluoroethylene (PTFE), polyethylene (PE) and paraffin [18].

To determine acidic and basic components of work of adhesion, we need already three liquids. A new computational algorithm was proposed for this purpose by Good and Hawa [27] as an improvement of their own work. Therein, the acceptor γ^+ and donor γ^- parameters are calculated as solution of a system of nine equations for nine unknowns by means of three polar liquids at three solid surfaces.

Then work of adhesion W_A can be calculated as follows:

$$W_A = 2\sqrt{\gamma_1^d \cdot \gamma_2^d} + 2\sqrt{\gamma_1^+ \cdot \gamma_2^-} + 2\sqrt{\gamma_1^- \cdot \gamma_2^+}.$$

The behaviour of liquids on smooth solid surfaces is rather well understood. However, for rough solid surfaces the situation is much less clear, even though roughness occurs on practically all real surfaces of engineering or biological interest. The contact water angle is widely used as a criterion for evaluating surface hydrophobicity/hydrophilicity. However, recognition of the importance of surface hydrophobicity is growing in various industries, such as those of glass, automobiles, and electronics. To date, the contact angle and contact-angle hysteresis (the difference between the receding contact angle and the advancing contact angle) have been commonly employed as criteria for assessing the hydrophobicity or hydrophilicity of solid surfaces. An extensive overview about several models for predicting wetting behaviour can be found in [28].

2 Contact Angle Measurements

Two methods proved to be useful for characterisation of surfaces—sessile drop method and Wilhelmy plate method [29]. With the sessile drop method, a drop of test liquid or of melt is placed on the solid. After reaching equilibrium, the contact angle is read on an enlarged picture of the resting drop. With the Wilhelmy plate method, a sample with well-determined geometry is dipped in the test liquid, then the contact angle is determined from the changes in force occurring in the process. This method is especially suitable to characterise wetting kinetics on fibres by polymer melt. Velocity and degree of fibre wetting by polymer melt can be directly followed, allowing consideration of the rheological aspect when characterising strength properties of actual composite materials.

2.1 Quasi-static Contact Angle Measurements

The *sessile drop method* is used to investigate wetting of pure liquids on real surfaces in order to characterize the solid surfaces, or of aqueous solutions of surfactants, polymers and other water-soluble substances on model solid surfaces in order to characterize the solutions. The measurement data are the contact angle θ, drop base "d" and drop height "h" of the drop as shown in Fig. 3.

In an effort to obtain a more precise description of the surface energy, measurements of advancing angle θ_A and receding angle θ_R are increasingly used. The difference between the advancing and the receding angle is referred to as *contact angle hysteresis* ($\theta_A - \theta_R$). The latter provides additional information on surface morphology and chemical composition as well as on surface roughness. However, it should be remembered that contact angle measurements only allow determination of changes as against the standard.

It is well known that the state of a surface affects crucially its wettability. Therefore, controlling the surface properties such as roughness, surface structure

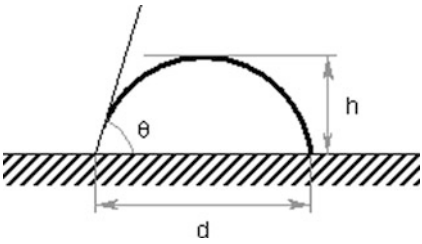

Fig. 3 Droplet "sitting" on a surface: sessile drop method

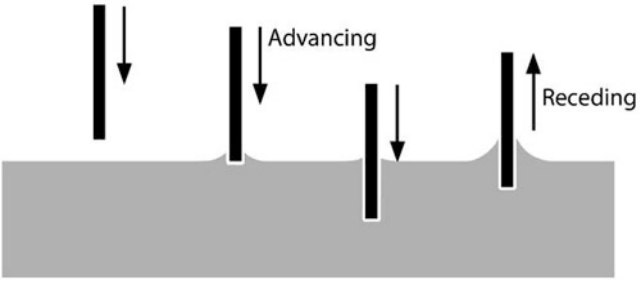

Fig. 4 Measurement of the advancing and receding contact angle of a fixed particle layer using the Wilhelmy plate method

and chemical composition is of great importance. Only in exceptional cases it is possible to infer the kind of surface alterations (roughness, chemical differences, charges, etc.) directly from contact angle alterations.

Advancing and receding contact angle measurements are possible force-driven if the drop volume will be increased or decreased. Since work of adhesion is by definition *reversible*, speaking in terms of thermodynamics, wetting and de-wetting should be identical, if there is enough time for balancing out the contact angle. There might not be any hysteresis if, beside van der Waals forces between liquid and solid surfaces (which are always present), no additional forces would participate in contact formation. Thus, a contact angle hysteresis can provide important information on molecular processes progressing at the interface (acid–base interactions).

An alternative method to evaluate wettability of a surface is to raise the liquid level gradually until it touches the handing plate or cylinder such as a single fibre suspended from a balance. The increase in weight is then noted, and this method is known as the *Wilhelmy plate technique*. The modified Wilhelmy plate method is gaining importance in view of the growing interest in determining the contact angles on nanoscalic materials—particles, fibres, nanotubes being added to polymeric compounds and other complex fluids [30, 31]. The principle of this method is balancing a thin plate immersed in liquid. If this technique is performed as a dynamic method, the partial contact angle values are attained reaching its maximum value—advancing contact angle θ_A, by immersing the plate into the liquid. If the plate is moved out of the liquid, receding contact angle θ_R is obtained (as shown in Fig. 4).

Based on the modified Wilhelmy plate method, wettability of porous media such as powders can be characterised by spontaneous capillary penetration of a liquid into pores spaces. Two experimental techniques are most commonly employed. The first one, height-time technique, see e.g. [32], measuring the height to which the liquid front advances in porous solids during the capillary rise process, and the second one, weight-time technique developed by Chwastiak [33], studying the increase in the weight of porous solids caused by the progression of the liquid inside their pores. In both cases, the experimental results were described by means of Washburn equation [34]. The literature on this topic is vast. The complex geometry of particle pore spaces creates numerous combinations of interfaces, capillaries, and wedges in which a liquid is retained, and results in a variety of air–liquid and solid–liquid configurations, making the interpretation of the results extremely difficult.

2.2 Dynamic Wetting Measurements

Contact angle as a thermodynamic equilibrium property, virtually all the published data for which reproducibility is claimed, are measurements of advancing contact angle within a minute of *three-phase contact* (TPC) line displacement. The second category is that of truly dynamic contact angles. If the TPC line as a phase boundary liquid–solid simultaneously moves relative to the adjacent solid surface, a dynamic contact angle will be observed. Dynamic contact angle means the contact angle as a function of time, which can significantly differs from the static contact angle.

Dynamic wetting measurements are possible either force-driven, if the drop volume will be increased/decreased or as time-dependent contact angle measurements with a constant volume. In the former case, advancing or receding angles[4] are formed to analyze the *contact angle hysteresis*, i.e. analysis of chemical and mechanical heterogeneities (as described in Sect. 2.1). In the latter case, the temporal contact angle change because of spontaneous spreading of the liquid is measured. If the spreading velocity is limited by the resistance of the TPC line, this phenomenon is referred to as *wetting dynamics* or *wetting kinetics* as shown in Fig. 5. The contact angle depending on the contact time of solid surface with measuring liquid is called *dynamic contact angle*.

For many applications, surfactants are introduced into the aqueous phase to increase the rate and uniformity of wetting. Despite their enormous technical importance, there is a lack of data in the literature about the spreading dynamics of aqueous surfactant solutions. The knowledge of how surfactant adsorption at the surfaces involved affects the spreading mechanism and dynamics is also limited. For more detail on wetting dynamics see [35–38]. Dynamic wetting measurements allow studying surfactants, polyelectrolytes or other surface-active substances as well as their mixtures and engineered surfaces [39].

[4]Strictly speaking, these are quasi-static measurements in the physical sense.

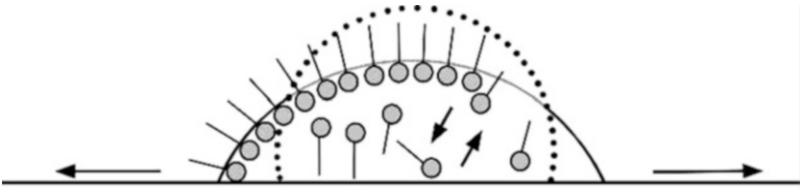

Fig. 5 A water drop containing surfactant molecules simultaneously spreading over a surface

3 Wetting Measurement in Technological Applications

Characterization of materials based on wetting measurements/interfacial thermodynamics is the most frequently used method in technological applications.

3.1 Fibre Wetting in Composite Processing

In fibre-reinforced composite processing, characterization of both—fibre surface properties and wetting behaviour of polymer on fibre is important [40]. From the experimentally determined contact angles of water, the surface free energies of fibre surface can be estimated using the equation of state for solid–liquid interfacial tension as described in Sect. 1.5. The modified Wilhelmy technique is also used to measure diameter of fibres [41].

Since the contact formation between fibre and matrix during composite processing occurs from the melt or solution, it is necessary to investigate fibre wettability for optimization of interfacial adhesion properties. Most thermoplastic polymers used in practice have a relatively high melting point, high softening temperature and high viscosity of the melt. This can cause an incomplete wetting of the reinforcing material by the melt and thus hamper the contact formation due to the fact that the actual contact zone becomes relatively small after the consolidation of the melt (the larger the contact area created the stronger the adherence). However, wetting measurements are indispensable as additional source of information for a comprehensive analysis of the interfacial properties of some practically relevant systems.

As described in [42], a Wilhelmy high-temperature wetting apparatus was used to study the adhesion between polymer blends and unsized glass fibres by determining the polymer melt wetting tension. The measurable quantity in the Wilhelmy experiment is the wetting tension $\gamma_L \cos\theta$ at the polymer melt/solid interface, which equals the force F per unit length of the perimeter p of the solid sample:

$$\gamma_L \cos\theta = \frac{F}{P} = \frac{g\Delta m}{p}$$

where γ_L is the surface tension of polymer melt, θ is contact angle, g is the gravitational constant, Δm is the change in mass before and after the fibre is immersed into the polymer melt. The high-temperature wetting apparatus [43] consists of a highly sensitive Sartorius microbalance (sensitivity of 1 μg), which is connected to a high-temperature cell through a stainless steel tube with an inner diameter 8 mm. The thin glass fibres used as solid probes are attached (using epoxy glue) to a metal wire, which is hooked onto another longer wire. The latter is fixed to the microbalance. In the high temperature cell the blends are heated under an inert gas flow. The temperature can be controlled with an accuracy of ±0.5°C. The polymer is brought into contact with the fibre by moving a motor-driven table at a constant velocity of 0.15 mm/min. The temperature in the cell, the velocity of the motor-driven table, recording of the change in mass by the microbalance before and after the fibre is immersed in the melt, and the atmosphere in the cell (inert gas pressure) are controlled by a computer. Before the fibre touches the polymer melt surface, its weight contribution is zeroed by the calibration routine of the balance. After the fibre has contacted the melt surface, the balance records the gain in weight caused by the wetting of the fibre.

The main difficulty in this experiment is the high viscosity of the polymer blend. Consequently, not only surface tension effects have to be considered in the Wilhelmy experiment but also hydrodynamic effects. Due to the forced fibre/liquid motion, non-negligible force contributions result from the shear stress exerted by the viscous flow of the liquid on the fibre. To exclude these hydrodynamic effects in wetting measurements, the fibre is held stationary at a constant penetration depth until viscous relaxation occurs. It is assumed that the meniscus of the liquid returns to equilibrium when a constant weight is reached. Only under these conditions, the measured force per unit length equals the wetting tension of the solid/polymer melt system. The fibre was immersed into the melt to a penetration depth of 0.15 mm. At this depth it was held stationary for 2 min, then the fibre was immersed to 0.30 mm depth and again held stationary for 2 min. At the last immersion stage, 0.45 mm depth was reached, glass fibre was held stationary for 5 min and after that it was emerged using the same sequence (0.15 mm/min emersion rate, two stops for 2 min each, at 0.30 and 0.15 emersion depths). Such immersion/emersion sequence allows polymer blend meniscus to relax, which results in a constant weight difference. Complete wetting was assumed when no weight difference was observed after the fibre was immersed and emerged at a given temperature. On average, the time required for one measurement was 30–45 min. A typical curve from a Wilhelmy balance experiment with the blends and a thin unsized glass fibre is shown in Fig. 6. Negligible weight differences between immersed and emerged states confirm a complete wetting mentioned above. This means that $\cos\theta = 1$ and surface tension of the blend γ_L (not wetting tension $\gamma_L \cos\theta$) was measured.

Temperature coefficients were determined from γ_L vs. T relationships as the slope of the curves.

In order to understand the processes that occur at the epoxy resin–polysulfone/glass fibre interface, surface tension of such blends was studied. The aim was to determine the temperature dependence of the blends surface

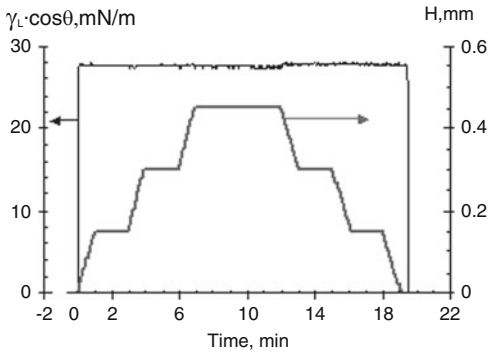

Fig. 6 Typical plot of wetting tension measurements obtained by the Wilhelmy technique for epoxy resin/polysulfone blends and unsized glass fibre ($d = 15.7\,\mu$m) at 190°C; H is the depth of fibre penetration. Reprinted from [42]

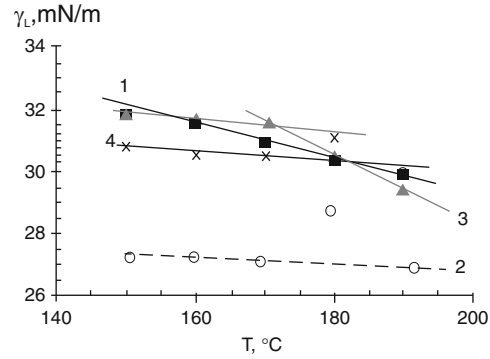

Fig. 7 Surface tension vs. temperature relationships for various epoxy resin–polysulfone systems. Polysulfone content: (1) 0 wt%, (2) 5 wt%, (3) 10 wt%, (4) 15 wt%. Reprinted from [42]

tension at the interface with glass fibres and how it was influenced by polysulfone concentration. It was found that surface tension decreases as the temperature increases which is quite typical for γ_L vs. T relationships and was already observed for different liquids, oligomers and highly viscous polymer melts. Temperature dependencies (Fig. 7) also contain information about the surface entropy, which is defined as $-(d\gamma_L/dT)$. It was found that incorporation of polysulfone significantly changed the surface entropy. In most cases, temperature coefficients of the blends were markedly lower than that of pure epoxy resin. It is also very interesting that incorporation of 5 wt% polysulfone resulted in the maximal decrease of $-(d\gamma_L/dT)$, while the surface entropies for the blend with 10 wt% modifier as well as that obtained for epoxy resin-15% polysulfone blend are closer to the $-(d\gamma_L/dT)$ value for epoxy resin. However, two $-(d\gamma_L/dT)$ values were obtained for epoxy resin-10% polysulfone blend. Its surface entropy, calculated for the 170–190°C temperature interval, is the highest, even when compared with the unmodified epoxy resin. It could be possibly explained by the unstable structure of the blends. It is assumed that the driving force for a good flow of a polymer is low viscosity, whereas for a good wetting of a substrate a low surface tension of the polymer is needed. In our case, the viscosity of the blends increased with polysulfone content increase which could possibly result in the retardation of the fibres impregnation

during composites production. On the other hand, surface tension values of the blends, except for 5 wt% polysulfone, were close to that of epoxy resin, so they should not lead to significant changes in the fibres wetting.

Overall conclusion of the studies can be drawn as follows, underlining the importance of wetting measurements in composite processing: A combination of wetting measurements based on the modified Wilhelmy plate method and rheological investigations in the system epoxy resin–polysulfone/glass fibre revealed that (1) activation energy for viscous flow as well as surface tension vs. polysulfone concentration relationships are nonadditive; (2) no significant changes in the kinetics of fibres wetting by the blends with increase in polysulfone content were observed; (3) all the ternary blends (epoxy resin–hardener–polysulfone) required at least 30 min at 180°C to achieve ultimate levels of the properties measured; (4) sea-island morphology of the blend with 5 wt% polysulfone and morphology with co-continuous phases in the case of blends with 10–15 wt% polysulfone were found after curing.

3.2 Wetting Studies on Human Hair

Dynamic penetration studies on differently modified human hair makes it possible to estimate the possibilities of water-soluble polymers to act as care components both in conventional shampoo formulations (free of the oil component) and in microemulsions. To estimate the spreading behaviour of water in terms of penetration rate, the capillary penetration method was used and improved. Methodological studies were accompanied by a study to determine water-absorbing capacity, water release by evaporation, topographic properties such as roughness and lustre of hair surfaces treated compared to the reference hair available as damaged (bleached) and undamaged.

The development was done with three different formulation concepts—a classical hair shampoo formulation, a micro emulsion based formulation and three market formulations claiming conditioning effects. Each formulation concept was represented by three different samples. The developed method is derived from a classical Washburn approach [34] originally developed to measure powder wetting. A bundle of parallel hair fibres in a measurement tube is connected to a micro balance. Water fills the measurement tube due to capillary effects once the hair gets in contact with the water and the weight of the tube increases. The weight increase over time is measured. It is dependent to the hydrophilic/hydrophobic properties of the surface. The influence of a hair care formulation on the surface of the hair can be detected by comparing untreated and modified hair samples.

The analysis can be made in an apparatus usually used for the measurements of surface tensions. The instrument has to offer a micro balance and the capability for time dependent measurements.

The hair of Asian type was purchased from Kerling International Haarfabrik in Backnang. Since healthy hair is by a sebum layer protected, hair under study was

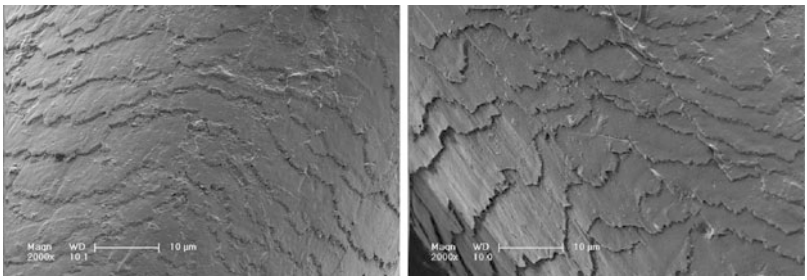

Fig. 8 SEM images of a reference hair (*left*) and a hair after bleaching (*right*)

damaged (roughened and hydrophilized) through bleaching in order to investigate the effect of individual polymer as additives in a care shampoo formulation. 10 ml of a 30% solution of H_2O_2 and 90 ml of a 30% solution of NH_3 were mixed. For deactivation of the mixture after hair bleaching $NaHSO_4$ was used. In Fig. 8, a reference hair as purchased and a hair after bleaching is shown.

The hair was cut into bundles of 10 cm lengths which are approximately two times longer than the measurement glass tubes. The hair was washed three times in a 1g/l solution of Marlipal 242/28 (Fatty alcohol-(C_{12}-C_{14})-polyethylene glycol-(2 EO)-ether sulphate sodium salt, INCl: sodium laureth sulfate) kindly provided by Sasol (Marl, Germany) in deionised water at 25°C (reference hair). After washing, the hair is reconditioned by pure deionised water until no traces of surfactant can be detected. Finally, the hair bundles are dried at 40°C in a vacuum oven for at least 2 h followed by drying overnight at room temperature.

For measurement glass tubes with an inner diameter of 2 mm and a length of 4 cm, hair portions of about 100 mg are separated. Every portion is arranged to a parallel hair bundle and pulled through the measurement glass tube with a sling. The hair is cut perpendicularly to the fibres at the bottom and the top ends of the glass tube. The hair bundle juts 3 mm out from the bottom end. The prepared measurement glass tubes are clearly marked and stored in a temperature-controlled laboratory maintained 24 ±1°C and 40 ±3% humidity.

A major drawback of the approach is the difficulty to get a constant packing (i.e. identical capillaries) in every glass tube especially with inhomogeneous fibres like human hair because small differences in the packing result in poor reproducibility of the experiments. Therefore, a calibration measurement with reference hair is required to scale measuring results to a comparable level. Thus, every tube is characterised by a calibration measurement with pure water. First, the weight of all filled glass tubes is determined. Then every sample is measured using the capillary rise technique according to the modified Washburn approach with deionised water. A typical graph for the weight vs. time curve is shown in Fig. 9.

The penetration rate is determined from the linear part of the weight vs. time curve by averaging at least 10 measurements. Next to the calibration measurement, the hair was reconditioned for the treatment with the hair care formulation. The measured sample is wetted completely with deionized water. After calibration,

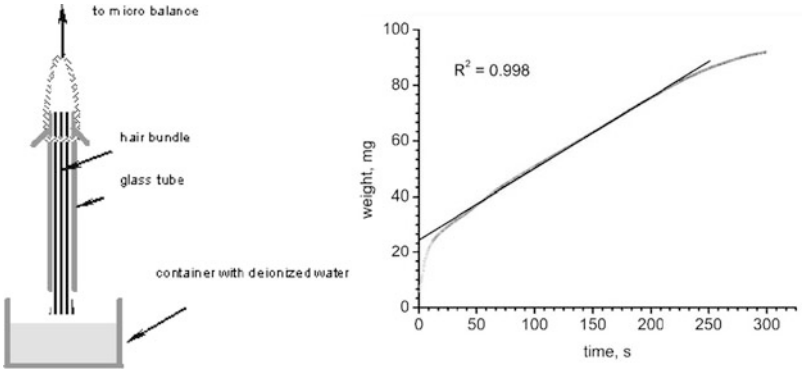

Fig. 9 Experimental set up (*left*) and single calibration measurement with pure water (*right*)

glass tubes are reconditioned at 40°C in an vacuum oven for 2 h followed by drying overnight at room temperature until the prior determined sample weight is reached again.

A solution of desired formulation was solved in deionized water to a concentration of 1 g/l. Each of 10 glass tubes is immersed into an usual test tube with 9 ml of the formulation solution for 30 min. After treatment, glass tubes containing hair bundles were rinsed several times with deionized water and dried according the drying procedure described above. The procedure was repeated 3 times until the surface tension of the rinsing water is identical with those of the pure water. Finally, the penetration rate of pure water is determined again as in the calibration procedure.

A comparison of the parameters investigated reveals that some polymers under investigation are well suitable as care components in a shampoo formulation. Moreover, it is possible to evaluate the influence of the oil component (paraffin, jojoba and silicone oil) in regard to the care effect. Jojoba and paraffin oil, in connection with the "care polymers" bring a positive effect for damaged hair, i.e. a considerable increase in the surface hydrophobicity, an improvement in lustre accompanied by surface smoothing and a time reduction in drying the hair. In the case of damaged hair, the conventional formulation with a care component gave better results than a micro-emulsion.

Additionally, contact angle of water on differently modified single hair was measured using the Wilhelmy plate method. In Fig. 10a, advancing and receding contact angles of pure water as well as their average values for reference hair were presented. In Fig. 10b, water contact angles as well as the water contact angle hysteresis for differently modified hair are summarized.

3.3 Wetting Measurements in Textile Characterization

It is well-known that the qualities of fabrics are closely dependent on their structure. Particularly, construction parameters, such as fineness of filaments and yarn, warp

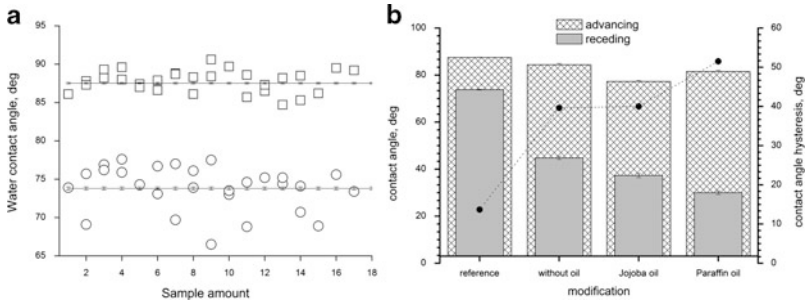

Fig. 10 Advancing and receding contact angles of water for reference hair cleaned with sodium laureth sulphate measured using the Wilhelmy plate method: the water advancing contact angle $\theta_A = 87.5°$ and the water receding contact angle $\theta_R = 73.8°$ (**a**), and contact angles for differently modified hair in comparison (**b**)

and weft density as well as the type of weave, control the texture and surface topography of fabrics. The fabric texture affects the porosity and strongly influences the textile characteristics such as fabric mass, thickness, draping ability, stress-strain behaviour or air permeability [44–46]. The surface topography of fabrics is responsible for their functionality—appearance and handle, wettability, soiling behaviour and cleanability [47, 48], abrasion resistance and wear [49]. There are very few systematic investigations of quantitative relations between construction parameters, topography of fabrics and their wettability, however.

The interaction between liquids and textile surfaces depends on the wettability of fibres, their surface geometry, the capillary geometry of the fibrous assembly, the amount and chemical nature of the liquid as well as on external forces. A randomly rough textile surface possesses pores, crevices, capillaries or other typical structures with their own characteristic wetting and penetration properties. As a consequence, the apparent contact angle on these surfaces will be affected by thermodynamics and kinetics associated with such intrinsic structures.

Wetting measurements in textile characterization are useful to evaluate changes before and after their modification in every respect. Dynamic contact angle measurements of aqueous surfactant and polymer solutions were used on textile surfaces in order to examine their soil-release properties [47, 48, 50].

Wetting measurements was used to estimate the degree of both, oily dirt sticking on the fabric after impregnation with different soil release polymers (SRP) and soil removal after washing. Cleanability of soiled textiles was evaluated as well by the soil additional density (SAD) analysis. The results demonstrated the application of dynamic wetting measurements in characterising both textile materials and interactions between them and aqueous solutions of soil release polymers. Differences between individual SRP were determined with respect to their spreading velocity on fabrics despite the similarity of their chemical composition and of the surface tension of their aqueous solutions. The weft-knitted double jersey fabric with the markedly higher filament fineness and surface porosity was found to show higher

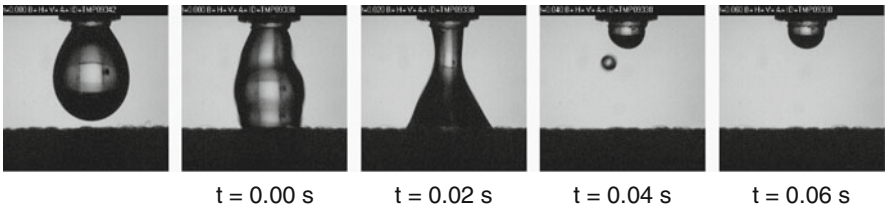

Fig. 11 Image sequence of a water drop applying to the surface of weft-knitted double jersey fabric treated with SRP [47]

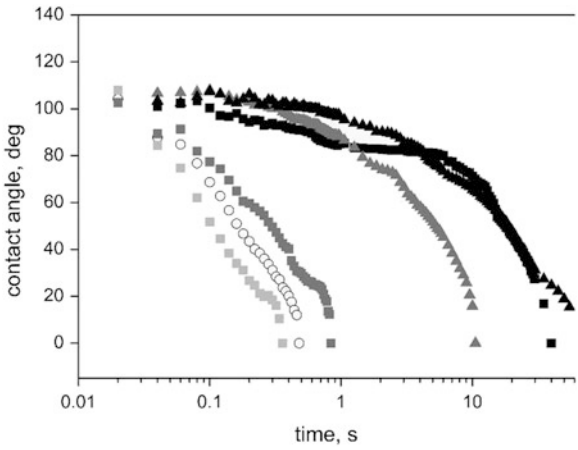

Fig. 12 Dynamic contact angles for the woven fabric F2 after soiling and washing with and without pre-treatment with SRP: (*circle*) untreated; (*light gray square*) after treatment with SRP; (*black square*) stained after treatment; (*gray square*) washed after treatment and staining; (*black triangle*) stained without treatment; (*gray triangle*) washed after staining without treatment

relative cleanability in soiling tests if treated with soil release polymers. In the case of untreated stained one, washing dramatically affects its cleanability (i.e. stain spreads over the whole surface) comparing with other textile materials.

The results for the spreading velocity (dr/dt) are conform with the data for the surface porosity for knitted fabrics: higher porosity leads to faster spreading. In the case of the woven fabric, the spreading velocity is, however, higher than that for knitted ones at comparable porosity, demonstrating the dependency of spreading characteristics on the kind of fabrics used. After treatment with SRP, recording of water contact angles was hardly possible due to complete hydrophilization of the fabrics surfaces. Figure 11 illustrates the image sequence of a water droplet applied to the surface of weft-knitted double jersey fabric treated with SRP. It is clearly seen that the water droplet completely penetrate into the textile surface after only 20 ms. Others SRP used show the same tendency.

Figure 12 shows (as an example) the dynamic water contact angles for a woven fabric. For the rather hydrophilic woven fabric, soiling hydrophobised its surface in both cases without and with pre-treatment with SRP. The fabric remains hydrophobic after its washing.

The SRP treatment of warp-knitted fabric and woven one also results in lowering their surface energy and improving their water absorptivity. The differences between

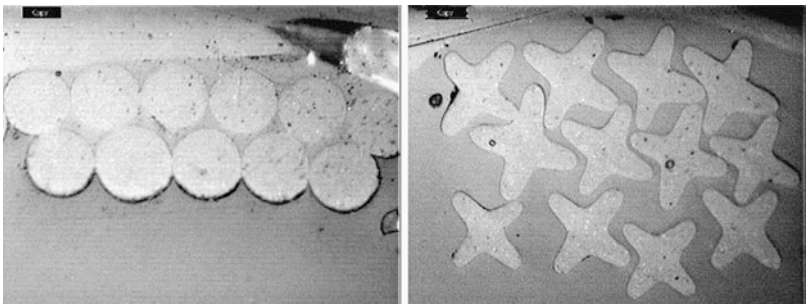

Fig. 13 Microscopic images of (cross-sectional view) of round (*left*) and cruciform (*right*) cross-sectional shaped filaments [51]

untreated and impregnated states were here, however, less marked than those for weft-knitted double jersey. It should be noted in this case, the weft-knitted double jersey fabric was made from textured "super-hydrophobic" properties to the fabric's surface.

In other studies [50–52], it was shown that the wetting, soiling and cleanability properties can be affected by using yarn of the same chemical nature with different structure and differently profiled polyester fibre, different types of weave and different weft density keeping the warp density constant. It is well known, that synthetic fibres which are predominantly spun by the melt spinning method with spinnerets having the non-circular hole geometry are called profiled or non-circular fibres. Various types of non-circular fibres have been developed to add functionalities and aesthetics to synthetic fibres leading to the change of their surface properties. The cross section of a synthetic fibre produced by the melt-spinning method can be easily varied by changes in the spinneret hole shape. In general, fibres consisting of non-circular cross-sectional shaped filaments show properties different from those of fibres with circular cross-sectional ones, including the bending stiffness, coefficient of friction, softness, lustre, comfort, pilling, bulkiness, handle, and performance. Microscopic images of different filament cross sections are illustrated in Fig. 13.

Variations in interlacing are also reflected in the fabric wettability considered in terms of the spreading rate as reported earlier [53]. The spreading rate decreased with increasing waviness for the plain weave, whereas it increased in the case of the twill one. It was concluded that the fabric wettability could be adjusted (in certain limits) by variation of density and interlacing keeping in mind the same chemical nature of microfilaments. Noticeable differences in the wetting behaviour of water are seen between the two types of weave if changes in porosity are considered. In the case of the plain weave, higher weft density leads to lower porosity and to higher water absorption time, as a consequence, shown in Fig. 14.

Moreover, water penetration into the plain texture is slightly slowed down with increasing porosity, reaches a maximum value of the absorption time (about 16 s) in the porosity range of approximately 1 $\mu m^3/\mu m^2$, and then accelerates towards the higher porosity values. It can be speculated about a "critical" value of the fabrics

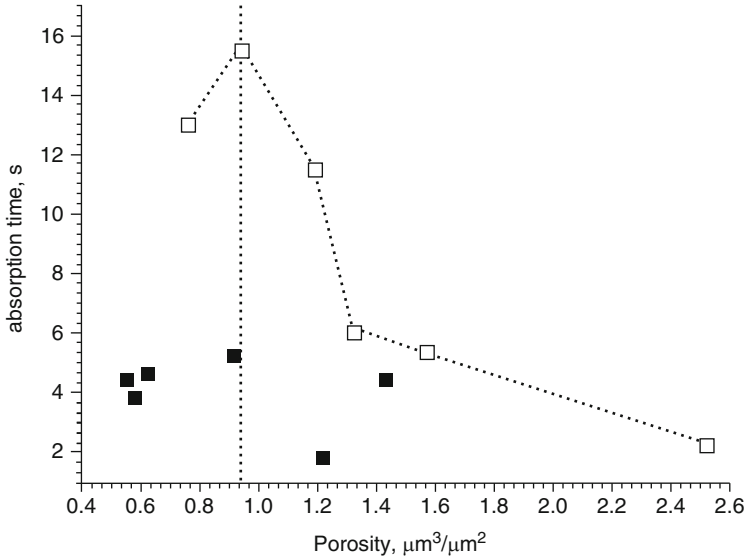

Fig. 14 Absorption time vs. surface porosity calculated as the ratio between the real pore volume and the corresponding geometric surface for (*white square*) plain and (*black square*) twill structures. Reprinted from [52], Copyright (2008), with permission from SAGE publications

porosity. Presumably, below this value water percolates with low velocity and above this with high a value. On the contrary, higher weft density of the twill weave results in higher porosity. The values of absorption time obtained for the twill texture are generally very low in about 2–5 s and almost independent of the porosity.

The differences in the penetration behaviour of water observed on two predetermined pattern of interlacing are caused by the different topographical structure since the chemical nature of filaments used was kept constant. It is noted, that the lateral distance between the threads is about 120 and 300 μm for the twill and plain weaves, respectively. The vertical dimension of the surface features is measured up to 20 μm for the plain topography and 40 μm for the twill topography. It is well known that in the case of moderately hydrophobic surfaces the complex internal geometry of real porous systems could enhance liquid penetration. The fabrics used were woven from polyester yarn. As reported earlier [35], this polymer is moderately hydrophobic with the water contact angle of 77° on its flat surface. The results obtained in the present study would suggest that water advanced in a stable flood (wicking regime) is observed [54]. The difference in the penetration behaviour (lower for the plain weave and faster for the twill weave) arises with the difference in the shape and size of the pores.

In essence, to achieve a more hydrophobic fabric texture, the technological parameters could be changed as follows: for both plain and twill structure, the weft density and filament fineness should be increased, and the yarn fineness should be reduced. Alternatively, the use of profiled fibres, e.g. cruciform, the fabric

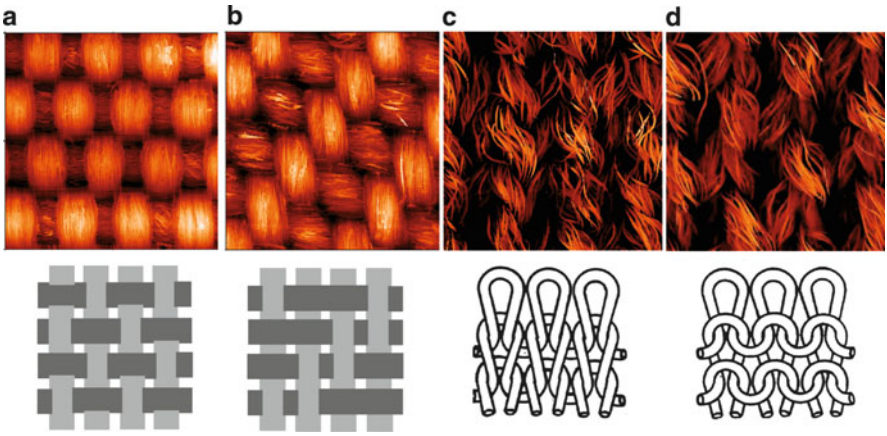

Fig. 15 Woven structures: (**a**) plain weave; (**b**) twill weave; and weft-knitted structures: (**c**) face side and (**d**) reversed side

manufacturing could lead to a more hydrophobic fabric texture on the basis of different roughness length scales [52].

An alternative method to evaluate the wettability of a textile surface is to raise the liquid level gradually until it just touches the hanging plate (or cylinder like single fibre) suspended from a balance. The increase in weight is then noted (cf. Sect. 2.1). Major advantages of the Wilhelmy plate technique are (1) the conditions of measurements are highly reproducible; (2) the speed of movement of the three-phase boundary is readily controlled; (3) the sensitivity of the technique is very high. Close agreement can be obtained between the Wilhelmy technique and careful measurements by the sessile drop technique. The plate method is especially useful when kinetic effects (adsorption, desorption, etc.) are important.

The liquid uptake measurements by means of the Wilhelmy plate technique were carried out with differently enzymatic treated fabrics of different type. A fabric sample is connected to a micro balance. Before the fabric sample touches the water surface, its weight contribution is zeroed by the calibration routine of the balance. After the fabric sample has penetrates into a liquid (defined depth of 1 mm), the balance records the gain in weight caused by the wetting of the textile and liquid uptake into the fabric due to capillary effects. Images of fabrics with the woven structure are illustrated in Fig. 15. The weight gain over time is measured. It is strongly dependent on the hydrophilic/hydrophobic properties of the surface. The influence of the fabrics modification can be detected by comparing differently modified samples. The liquid uptake rate is determined from the linear part of the mass square vs. time curve by averaging at least 3 measurements. The measurements were carried out with water and paraffin oil.

Comparing water and oil uptake rates with fabric surface topography parameters (roughness, surface porosity), it is possible to conclude about the effectiveness of

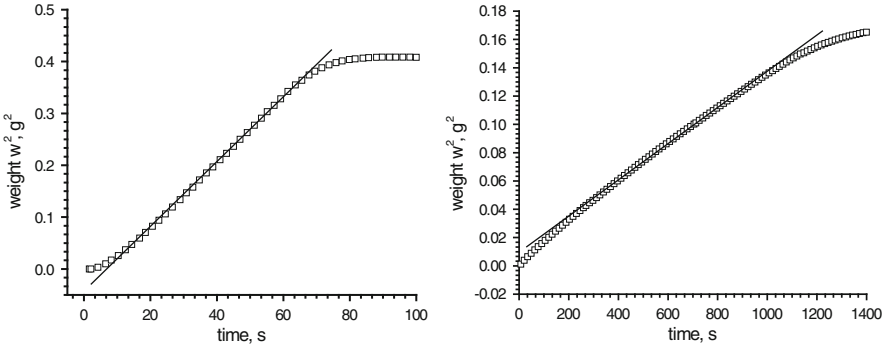

Fig. 16 Water (*left*) and paraffin oil (*right*) uptake rate of plain weaved fabric

modification in respect to cleanability and water evaporation capacity, i.e. drying rate.

A comparative analysis between different ether carbon acids with respect to wettability of fabrics, surface topography parameters and mechanical treatment by abrasion was done using the modified Wilhelmy plate method. To estimate the degree of hydrophobicity of textile surfaces before and after impregnation with protective finishes, dynamic wetting measurements were carried out with a dynamic absorption and contact angle tester. The water uptake rate is determined according to Washburn from the linear part of the mass square vs. time curve as shown in Fig. 16. Surface topography of fabrics was examined using an imaging measuring instrument for the optical analysis of roughness, MicroGlider (FRT, Germany), operating on principle of chromatic abberation. The measuring method was described in more detail in [47].

In Fig. 16, water and oil uptake is shown.

Some topography parameters such as mean roughness depth (Rz) and surface porosity (porosity of fibre surfaces without spaces between fibres) were obtained from the images with a size of 1 mm × 1 mm. The porosity is calculated as the ratio between the real pore volume and the corresponding geometric surface excluding spaces between fibres.

After impregnation of polyester materials with protective finishes carried out through immersion of these in the corresponding aqueous protective finish solution for 5 min, polyester fabrics were abrasively treated by using an abrasion test instrument APG 1000 (Maag Flockmaschinen, Germany). After abrading, wettability and surface topography of tested fabrics were re-examined (Table 3).

The modification of knitted fabrics with a finishing agent leads to a significant increase of the porosity, which is threefold higher for their unmodified face side than that for the modified one. Comparing macroscopic roughness parameters obtained for the modified twill woven fabric, a decrease is ascertain after its mechanical treatment by abrasion, and vice versa for the plain one. Differences between changes in roughness of three polyester textile materials with different initial topographic

Table 3 Topography parameters for fabrics used before and after abrading

	Surface porosity, $\mu m^3/\mu m^2$		
Type of fabrics	Unmodified	Modified with 2, before abrading	Modified with 2, after abrading
Plain	1.2	0.6	1.9
Twill	0.7	1.2	0.9
Knitted, face side	1.8	5.4	1.9
Knitted, reversed side	2.1	2.4	2.2

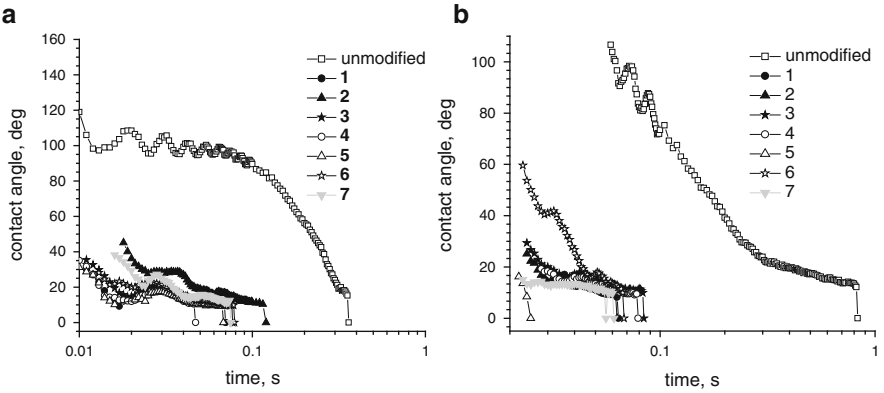

Fig. 17 Dynamic water contact angle for differently modified fabrics: (**a**) before their abrading; (**b**) after their modification by abrasion

structures being modified with a protective finish being ether carboxylic acid (isotridecanol ethoxylated carboxymethylated with pH 2.94 and surface tension of 26.4 mN/m) before and after their mechanical abrasion were determined despite the similarity of their chemical nature in the case of the soiling behaviour of such fabrics.

Figure 17a shows water contact angles for the fabrics before and after impregnation with different ether carbon acids (7 different substances obtained by Sasol Germany, Marl detailed in [49]) as measured using sessile drop method. The treatment of fabrics with these finishing agents results in lowering their water absorptivity. No significant differences were seen between different finishes with respect to hydrophilization of the fabrics. Water dynamic contact angles for unmodified fabrics and after their mechanical abrading are shown in Fig. 17b. A decrease of the water contact angle for unmodified fabrics indicates dramatic decreasing their abrasion resistance. Obviously, fabrics abrading, especially for knitted fabrics, results in increasing porosity followed by changing the wetting behaviour from highly hydrophobic to penetrating one.

Water uptake rate of the fabrics measured before and after abrading are summarized in Table 4 for the fabrics used. Interestingly, water penetrates fourfold faster

Table 4 Water uptake rate for differently modified fabrics before and after their abrading

	Water uptake rate $\times 10^5$, g^2/s						
	Before abrasion test			After abrasion test			
						Knitted	
♯	Plain	Twill	Knitted	Plain	Twill	f	l
0	0.04	0.15	1.84	8.01	1.39	99.83	174.0
1	0.03	0.02	1.71	0.60	0.71	5.96	23.17
2	0.04	0.02	9.97	0.65	1.0	120.0	151.0
3	0.03	0.06	35.4	8.79	10.0	254.0	140.0
4	0.01	0.01	0.34	7.79	7.59	5.46	33.95
5	0.1	0.06	20.8	0.69	1.7	112.0	137.0
6	0.1	0.14	53.4	7.68	1.36	314.0	492.0
7	0.002	0.02	0.73	7.84	7.63	270.0	160.0

(f) after abrading the face side of knitted fabric; (r) after abrading the reversed side of knitted fabric

into the woven fabric than into the knitted fabrics. The difference in the penetration behaviour arises from the difference in the shape and size of pores. From water uptake results, which are in agreement with dynamic contact angle measurements, the finishing agent **1** is the "best" for woven fabrics with the twill type of weave.

The finish **2** is also suitable with respect to changes in the wettability after abrading: the changes will be marginal. For knitted fabrics, the finish agents **1** and **4** seem to be the most suitable. From the contact angle measurements, the finishes **4** and **5** were obtained to be appropriate for this kind of polyester fabrics. In contrary to the wetting results describe above, the most suitable protective finishes for woven fabrics with the plain type of weave are not **3** and **7**, but **1**, **2** and **5**.

As differences between the wetting characteristics obtained from water uptake measurements are larger than those from the dynamic contact angle measurements, the water uptake rate seems to be more significant in estimating the "best" finishing agent. For all fabrics, the "best" finishing agent was revealed to be **1** in respect of changing the wetting characteristics.

The mechanical treatment of the fabrics by abrasion results in a decrease in hydrophilicity due to fuzzing (also called fuzzy and hairy, is a fabric condition characterized by a hairy appearance due to broken fibres or filaments.) caused by abrasive testing. To prevent unwanted changes in appearance of the fabrics usually occurring during washing, cleaning or in wear, fabrics can be modified with the following protective finishes: for plain woven fabrics, the finishing agents **3** and **7** would be the most suitable; for twill woven fabrics, the finishes **1** and **7** seems to be the "best"; for knitted fabrics, the finishes **4** and **5** can be used for modification. This analysis was done by assuming the slightest changes in fabrics wettability compared before and after abrading. A significant decrease of wettability indicates that some fuzzing defects appeared. A significant increase of wettability might be caused by gaping defects caused by irregular shrinkage of the yarns due to abrasive testing.

To explore the influence of different ether carboxylic acids provided by Sasol Germany as spin finishes for polyester fibres as well as protective finishes for

polyester fabrics, friction coefficient of polyester yarn produced by melt-spinning process and abrasion resistance of fabrics, respectively, were determined.

From friction measurements of fibre against steel, the spin finish **2** (Isotridecanol ethoxylated carboxymethylated) is evaluated as "the best" among other finishing agents with respect to decreasing the fibre friction.

The influence of textiles surface properties such as their topographical structure and degree of hydrophobicity on spreading and penetration behaviour of water before and after treatment with protective finishes as well as before and after mechanical treatment by abrasion was investigated.

The dynamic wetting and water uptake measurements were carried out to check the wetting characteristics of differently modified fabrics—impregnated with protective finishes and mechanically abraded. From these measurements, the water uptake rate seems to be a suitable parameter to estimate the abrading degree. The time of total absorption of water from the dynamic contact angle measurements as a wetting measure indicates changes in absorbing capacity after modification of fabrics with different protective finishes. The results described in this study support the usefulness of imaging techniques based on the principle of chromatic aberration as well as wetting measurements in characterising the surface of textile materials before and after their surface modification.

3.4 Wettability of Engineered Nanoparticles

A conceptually new methodology to collect information about wetting properties of technologically relevant nanoparticles using the Wilhelmy plate method along with modern optical techniques for surface roughness analysis is presented in brief. The results are based on several differently modified synthetic alumina particles as sun blockers for sunscreen products.

Emulsions are common formulation concepts employed to build stable systems consisting of two immiscible or partly immiscible liquids. They can be formed and stabilized only in the presence of well selected surfactants, polymers, proteins and their mixtures. Traditionally, surfactants composed of a hydrophilic and a hydrophobic part within the same molecule are used as emulsifiers. With increasing legal and consumer requirements to the emulsifiers being non-toxic, biodegradable, mild to skin and mucous, and with an attractive price/performance ratio, degrees of freedom in selecting and designing classical emulsifiers are limited. Consequently, industries such as cosmetics and pharmaceutics with high standards for product safety are seeking for alternatives to the conventional formulation concepts.

A new alternative approach uses nanoparticles according to the well-known principle of Pickering [55]. Especially, for products which contain particles in their formulation an additional or even complete stabilization by these particles will be a new and interesting concept. The key factor for the use of particles as stabilizing agent is their wetting by the two phases, namely the oil and aqueous phase. However, the affinity to each of the two phases should be different and is

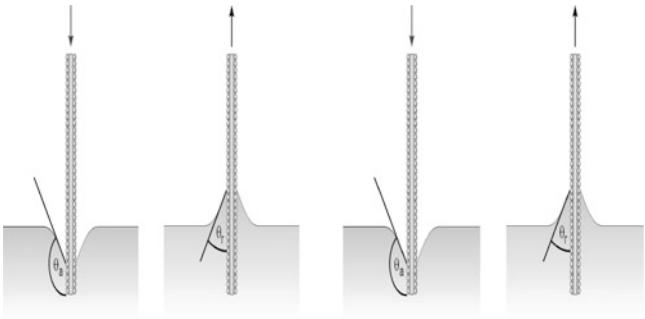

Fig. 18 Measurement of the advancing (*left*) and receding (*right*) dynamic contact angle of a fixed particle layer using the Wilhelmy plate method

expressed by the contact angle. The contact angle is an excellent measure describing the wettability of particles and their affinity interacting with liquids. Furthermore, it affects the stability of the emulsion through the energy of attachment in particles at the interfaces. In general, factors that affect surface chemistry and contact angles, will impact the stability and characteristics of the emulsion [56, 57].

Wettability of powders can be characterized by spontaneous capillary penetration of a liquid into pore spaces, however, the complex geometry of particle pore spaces creates numerous combinations of interfaces, capillaries, and wedges in which a liquid is retained, and results in a variety of air–liquid and solid–liquid configurations, making the result interpretation extremely difficult.

Pickering emulsions require sufficiently small particles which are usually at least tenfold smaller in size than the dispersed droplets of the emulsion. However, existing methods to characterize the particle wettability such as microsphere tensiometry, film and gel trapping techniques, and drop shape analysis fail in view of such small particles all with a similar size of less than 200 nm. In this study, wetting properties of differently modified alumina nanoparticles have been investigated by means of the modified Wilhelmy plate. This method seems to be suitable for a quick wettability characterization, and, therefore, this method may become a significant surface analytical tool in analyzing interfacial properties of powder materials.

Dispersible colloidal Boehmite alumina powders are used in this study, which are manufactured by Sasol (Brunsbüttel, Germany). The aluminas were modified by the manufacturer with *p*-toluene sulfonic acid (**1**) and alkylbenzene sulphonic acid (**2**). The surface coverage by two various modifying agents, the size of powder particles as well as of their primary aggregates in dispersion was investigated earlier in [58].

Water contact angles were measured to obtain the wettability of unmodified and modified alumina powders by the modified Wilhelmy plate method illustrated in Fig. 18.

The modified Wilhelmy plate method is gaining importance in view of the growing interest in determining the contact angles on nanoscalic materials—particles, fibres, nanotubes being added to polymeric compounds and other complex

Table 5 Values of advancing contact angles measured by the modified Wilhelmy method and sessile drop method as well as the ones corrected

		Modified Wilhelmy plate		Sessile drop method	
Particle type	Wenzel factor	θ, measured	θ, corrected	θ, measured	θ, corrected
1	1.994	18	62	10	60
2	3.815	54	81	91	90

Fig. 19 Topography images of modified plates (*left*) and (*right*) with particles **1** and **2**, respectively

fluids [30, 31]. The principle of this method is balancing a thin plate immersed in liquid. If this technique is performed as a dynamic method, the partial contact angle values are attained reaching its maximum value—advancing contact angle, by immersing the plate into the liquid. If the plate is moved out of the liquid, receding contact angle is obtained. In our measurements, alumina powders were attached to a double-sided adhesive tape. The measurements are performed at room temperature with deionized water. The air contained in pores cannot be displaced, as the plate roughness governed by attached particles is unavoidable, therefore, several immersion-emersion cycles were carried out. The receding contact angle seems to be more reliable because of its invariability during three measuring cycles. In addition, quasi-equilibrium contact angels were measured using the sessile drop method shown in Table 5.

The contact angle values measured using both methods seem to be underestimated because of the plate roughness, actually desired. The water-in-oil (W/O) a type of stable Pickering emulsion achieved using particles **2** cannot be explained with values lower than 90°. Assuming the Wenzel regime [59] during wetting, values measured were corrected using the Wenzel roughness factor $r_s = \cos\theta_{measured} / \cos\theta_{smooth}$. This factor was estimated from topographic images, shown in Fig. 19, taken with an image measuring instrument for the optical analysis of roughness MicroGlider (FRT, Germany). The roughness factor of a surface is the ratio between the real surface area and the geometric one. The correction of the measured contact angles with the roughness factor includes the assumption that the measured surface is completely wet, up to the scale of it' resolution. It is obvious that the determined roughness factor is bound by the resolution of the measuring device.

It is known that Wenzel regime is often not favoured energetically in the case of wet surfaces with roughness on many different length scales. It is likely that air is trapped in grooves of the surface and only a fraction of the surface comes into contact with the liquid. This case is referred to as the Cassie state [60]. It was shown

that the incomplete liquid–solid contact is driven by the surface slope [61]. Below a certain critical slope that depends on the true flat surface contact angle, Wenzel regime is favoured whereas above that value the Cassie state prevails.

Hence, slope distribution of the measured surface should be taken into account for further corrections of the measured contact angle on rough surfaces in order to determine wetting properties of the powder particles.

A theory for wetting was presented recently considering a Gaussian random surface [62]. Within the theory the average slope as well as the roughness factor are determined by the same parameter that is connected with the surface roughness power spectrum.

The results described above demonstrate the application of wetting measurements by the modified Wilhelmy plate in characterising dispersible colloidal powders. The difference between unmodified and modified alumina particles were determined with respect to their hydrophobicity/hydrophilicity. Analysing this in comparison with other properties of particles such as their electrical surface properties, the particle size in the dry and wetted states, and in an aqueous suspension, is an important factor in a development and mechanistic understanding the stability of emulsions.

References

1. Gibbs, J.W.: Trans. Conn. Acad. **3**, 108 (1873)
2. Rusanov, A.I., Shchekin, A.K.: Kolloidn. Zh. **61**, 437 (1999)
3. Young, T.: Philos. Trans. R. Soc. Lond. **95**, 65 (1805)
4. Weidenhammer, P., Jacobasch, H.-J.: Macromol. Symp. **126**, 51 (1997)
5. Churaev, N.V.: Adv. Colloid Interfacial Sci. **58**, 87 (1995)
6. Churaev, N.V.: Kolloidn Zh. **58**, 725 (1996)
7. Derjaguin, B.V., Churaev, N.V., Muller, V.M.: Surface Forces. Nauka, Moskau (1985)
8. Starov, V.M., Velarde, M.G., Radke, C.J.: Wetting and Spreading Dynamics. Taylor and Francis, Boca Raton (2007)
9. Fowkes, F.M.: J. Adhes. Sci. Tech. **1**, 7 (1987)
10. Owens, D.K., Wendt, R.C.: J. Appl. Polym. Sci. **13**, 1741 (1969)
11. Kwok, D.Y., Neumann, A.W.: Adv. Colloid Interface Sci. **81**, 167 (1999)
12. Good, R.J.: J. Colloid Interface Sci. **59**, 398 (1977)
13. Nardin, M., Schultz, J.: Compos. Interfaces **1**, 177 (1993)
14. Derjaguin, B.V.: Kolloidn. Zh. **69**, 155 (1934)
15. Derjaguin, B.V., Lazarev, W.: Kolloidn. Zh. **69**, 11 (1934)
16. Jacobasch, H.-J., Freitag, K.-H.: Acta Polym. **30**, 453 (1979)
17. Jacobasch, H.-J.: Oberflchenchemie faserbildender Polymerer. Akademie, Berlin (1984)
18. Berg, J.C.: Role of acid-base interactions in wetting and related phenomena. In: Berg, J.C. (ed.) Wettability, pp. 75–148. Marcel Dekker, New York (1993)
19. Good, R.J., van Oss, C.J.: The modern theory of contact angles and the hydrogen bond components of surface energies. In: Schrader, M.E., Loeb, G. (eds.) Modern Approach to Wettability: Theory and Applications, pp. 1–27. Plenum, New York (1991)
20. Good, R.J.: Contact angle, wettability, and adhesion: a critical review. In: Mittal, K.L. (ed.) Contact Angle, Wettability and Adhesion, pp. 3–36. VSP, Utrecht (1993)

21. Gutmann, V.: The Donor-Acceptor Approach to Molecular Interactions. Plenum, New York (1983)
22. Israelachvili, J.N.: Intermolecular and Surface Forces. Academic, San Diego (1991)
23. Good, R.J., Chaudhury, M.K.: Theory of adhesive forces across interfaces. 1. The Lifshitz-van der Waals component of interaction and adhesion. In: Lee, L.-H. (ed.) Fundamentals of Adhesion, pp. 137–150. Plenum, New York (1991)
24. Berlin, A.A., Bassin, B.E: Basics of Adhesion of Polymers. Chimia, Moskau (1974)
25. Kinloch, A.J.: Adhesion and Adhesives: Science and Technology. Chapman & Hall, London (1987)
26. Dutschk, V.: Surface forces and their contribution to adhesion and adherence in glass fibre reinforced polymer composites. Ph.D. thesis, University of Technology Dresden (2000)
27. Good, R.J., Hawa, A.K.: J. Adhes. **63**, 5 (1997)
28. Asthana, R., Sobczak, N.: J. Mater. **52**, 40 (2000)
29. Wilhelmy, L.: Ann. Phys. Chem. **CXIX**(6), 202 (1863)
30. Bachmann, J., Horton, R., van der Ploeg, R.R., Woche, S.: Soil Sci. Soc. Am. J. **64**, 564 (2000)
31. Kvítek, L., Pikal, P., Kovaříková, L., Hrbáč, J.: Acta Univ. Palacki. Olomuc. Chem. **41**, 27 (2002)
32. Good, R.J.: J. Colloid Interface Sci. **42**, 473 (1973)
33. Chwastiak, S.: J. Colloid Interface Sci. **42**, 298 (1973)
34. Washburn, E.W.: Phys. Rev. **17**, 273 (1921)
35. Dutschk, V., Sabbatovskiy, K., Stolz, M., Grundke, K., Rudoy, V.: J. Colloid Interface Sci. **267**, 456 (2003)
36. Dutschk, V., Breitzke, B.: Tenside Surfactants Deterg. **42**, 82 (2005)
37. Slavchov, R., Heinrich, G., Dutschk, V., Radoev, B.: Colloid Surf. A **354**, 252 (2009)
38. Lee, K.S., Ivanova, N., Starov, V.M., Hilal, N., Dutschk, V.: Kinetics of wetting and spreading by aqueous surfactant solutions (Review). Adv. Colloid Interfaces Sci. **144**, 54–65 (2008)
39. Dutschk, V.: Wetting dynamics of aqueous solutions on solid surfaces. In: Miller, R., Liggieri, L. (eds.) Drop and Bubble Interfaces, vol. 2. Progress in Colloid and Interface Science. Brill, Leiden (2011)
40. Plonka, R., Mäder, E., Gao, S.L., Bellmann, C., Dutschk, V., Zhandarov, S.: Compos. Part A **35**, 1207 (2004)
41. Bismarck, A., Kumru, M.E., Springer, J.: J. Colloid Interface Sci. **210**, 60 (1999)
42. Brantseva, T., Gorbatkina, Yu., Dutschk, V., Vogel, R., Grundke, K., Kerber, M.L.: J. Adhesion Sci. Technol. **17**, 2047 (2003)
43. Grundke, K., Uhlmann, P., Gietzelt, T., Redlich, B., Jacobasch, H.-J.: Colloids Surf. A **116**, 93 (1996)
44. Potluri, P., Parlak, I., Ramgulam, R., Sagar, T.V.: Comp. Sci. Technol. **66**, 297 (2006)
45. Milasius, V., Milašius, R., Kumpikaite, E., Olauškine, A.: Fibres Text. East. Eur. **11**, 48 (2003)
46. Kumpikaite, E.: Fibres Text. East. Eur. **15**, 35 (2007)
47. Calvimontes, A., Dutschk, V., Breitzke, B., Offermann, P., Voit, B.: Tenside Surfactants Deterg. **42**, 17 (2005)
48. Calvimontes, A., Dutschk, V., Koch, H., Voit, B.: Tenside Surfactants Deterg. **42**, 210 (2005)
49. Dutschk, V., Myat, S., Märtin, J., Stolz, M., Breitzke, B., Cherif, Ch., Heinrich, G.: Tenside Surfactants Deterg. **44**, 348 (2007)
50. Hasan, M.M.B., Dutschk, V., Calvimontes, A., Hoffmann, G., Heinrich, G., Cherif, Ch.: Tenside Surfactants Deterg. **45**, 274 (2008)
51. Hasan, M.M.B., Dutschk, V., Brünig, H., Mäder, E., Häußbler, L., Häßbler, R., Cherif, Ch., Heinrich, G.: J. Appl. Polym. Sci. **111**, 805 (2008)
52. Hasan, M.M.B., Calvimontes, A., Synytska, A., Dutschk, V.: Text. Res. J. **78**, 996 (2008)
53. Calvimontes, A., Synytska, A., Dutschk, V., Bell, Ch., Lehmann, B.: Melliand English **1–2**, E16 (2006)
54. Kissa, E.: Text. Res. J. **66**, 660 (1996)
55. Pickering, S.U.: J. Chem. Soc. **91**, 2001 (1907)
56. Lagaly, G., Reese, M., Abend, S.: App. Clay Sci. **14**, 83 (1999)

57. Melle, S., Lask, M., Fuller, G.G.: Langmuir **21**, 2158 (2005)
58. Dutschk, V., Stöckelhuber, K.-W., Albrecht, V., Geißbler, U., Simon, F., Petzold, G., Bellmann, K.: In: PARTEC2007, Proceedings, Nuremberg, 27–29 March 2007
59. Wenzel, R.N.: Ind. Eng. Chem. **28**, 988 (1936)
60. Cassie, A.B.D., Baxter, S.: Trans. Faraday Soc. **40**, 546 (1944)
61. Johnson, R.E., Dettre, R.H.: Adv. Chem. Ser. **43**, 112 (1964)
62. Yang, C., Tartaglino, U., Persson, B.N.J.: Eur Phys. J. E **25**, 139 (2008)